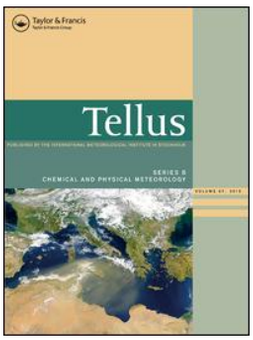

Tellus B: Chemical and Physical Meteorology

ISSN: (Print) 1600-0889 (Online) Journal homepage: http://www.tandfonline.com/loi/zelb20

# Characterization of the planetary boundary layer during SAMUM-2 by means of lidar measurements

Silke Groß, Josef Gasteiger, Volker Freudenthaler, Matthias Wiegner, Alexander Geiß, Alexander Schladitz, Carlos Toledano, Konrad Kandler, Matthias Tesche, Albert Ansmann & Alfred Wiedensohler

**To cite this article:** Silke Groß, Josef Gasteiger, Volker Freudenthaler, Matthias Wiegner, Alexander Geiß, Alexander Schladitz, Carlos Toledano, Konrad Kandler, Matthias Tesche, Albert Ansmann & Alfred Wiedensohler (2011) Characterization of the planetary boundary layer during SAMUM-2 by means of lidar measurements, Tellus B: Chemical and Physical Meteorology, 63:4, 695-705, DOI: 10.1111/j.1600-0889.2011.00557.x

**To link to this article:** https://doi.org/10.1111/j.1600-0889.2011.00557.x



Published online: 18 Jan 2017.

Tellus SERIES B CHEMICAL AND PHYSICAL METEOROLOGY
PUBLISHED BY THE INTERNATIONAL METEOROLOGICAL INSTITUTE IN STOCKHOLM

*Tellus (2011), 63B, 695–705*
*Printed in Singapore. All rights reserved*



TELLUS

# Characterization of the planetary boundary layer during SAMUM-2 by means of lidar measurements

*By* SILKE GROß[1,*], JOSEF GASTEIGER[1], VOLKER FREUDENTHALER[1], MATTHIAS WIEGNER[1], ALEXANDER GEIß[1], ALEXANDER SCHLADITZ[2], CARLOS TOLEDANO[1,†], KONRAD KANDLER[3], MATTHIAS TESCHE[2], ALBERT ANSMANN[2] and ALFRED WIEDENSOHLER[2], [1]*Meteorological Institute, Ludwig–Maximilians–Universität, Theresienstr.37, 80333 Munich, Germany;* [2]*Leibniz Institute for Tropospheric Research, Permoserstr.15, 04318 Leipzig, Germany;* [3]*Institute for Applied Geosciences, Technical University Darmstadt, Darmstadt, Germany*

(Manuscript received 11 November 2010; in final form 23 May 2011)

ABSTRACT

Measurements with two Raman-depolarization lidars of the Meteorological Institute of the Ludwig-Maximilians-Universität, München, Germany, performed during SAMUM-2, were used to characterize the planetary boundary layer (PBL) over Praia, Cape Verde. A novel approach was used to determine the volume fraction of dust $\upsilon_d$ in the PBL. This approach primarily relies on accurate measurements of the linear depolarization ratio. Comparisons with independent in situ measurements showed the reliability of this approach. Based on our retrievals, two different phases could be distinguished within the measurement period of almost one month. The first (22–31 January 2008) was characterized by high aerosol optical depth (AOD) in the PBL and large $\upsilon_d > 95\%$. During the second phase, the AOD in the PBL was considerably lower and $\upsilon_d$ less than ~40%. These findings were in very good agreement with ground based in situ measurements, when ambient volume fractions are considered that were calculated from the actual measurements of the dry volume fraction. Only in cases when dust was not the dominating aerosol component (second phase), effects due to hygroscopic growth became important.

## 1. Introduction

The planetary boundary layer (PBL) is the lowermost part of the troposphere, directly influenced by the Earth's surface. Its height varies strongly in time and space and can extend from a few hundred meters to a few kilometres (Stull, 1988). Aerosols found in the PBL typically show a large variability, e.g. with respect to the type, and the concentration of the aerosols. To improve our knowledge of the structure and extension of the boundary layer, numerous research activities have been pushed by modern remote sensing techniques (Schwiesow, 1984). Already in 1977 Kunkel et al. showed the potential of lidar systems for boundary layer studies, as they can determine the vertical distribution of aerosols and distinguish between different aerosol layers. Further studies, e.g. on convection in the PBL (Melfi et al., 1985), PBL-height (Strawbridge and Snyder, 2004, Wiegner et al., 2006), humidity fluxes (Kiemle et al., 1997) and wind in the PBL (Hooper and Eloranta, 1986) followed. Matthias and Bösenberg (2002) used regular lidar data to establish an aerosol climatology of the PBL over Hamburg, and Murayama et al. (1999) analysed the effects of dust and sea-salt in the PBL by means of lidar depolarization measurements.

In this work we present lidar measurements of the Meteorological Institute (MIM), of the Ludwig-Maximilians-Universität (LMU), Munich, Germany, of aerosol optical properties in the PBL taken during the second field campaign of the Saharan Mineral Dust Experiment (SAMUM). The measurement site was located at the airport of Praia (14.92°N, 23.49°W, 75 m above see level), the capital of the Cape Verde Islands in the Atlantic Ocean 500 km off the coast of Africa. The distance of the site to the eastern coast of the island was about 1000 m and about 4000 m to the southern coast of the island. It was free of buildings, vegetation or orographical barriers. Measurements were performed in January and February 2008. During this time of the year the Cape Verde Islands are mainly influenced by an easterly flow, advecting occasionally dust-loaded air-masses from the African continent and marine aerosols from the Atlantic Ocean.

*Corresponding author.
e-mail: silke.gross@ physik.uni-muenchen.de
†Now at: Group of Atmospheric Optics, Valladolid University, Spain.
DOI: 10.1111/j.1600-0889.2011.00557.x

The lidar derived optical properties discussed in this paper include the aerosol optical depth (AOD), the lidar ratio ($S_p$), and the particle linear depolarization ratio ($\delta_p$) at wavelengths $\lambda = 355$ and 532 nm, with the only exception that $S_p$ at 532 nm was not available during January. Furthermore, based on the lidar measurements we determine the volume-concentrations of Saharan dust and sea-salt particles in the PBL, that means, sort of a mixing ratio of dust and sea-salt was derived. The characterization of the PBL during this campaign is important as it provides a link between column-integrated measurements (Toledano et al., 2011), ground based measurements (e.g. Schladitz et al., 2011a,b, Kandler et al., 2011a,b) and airborne in situ measurements (e.g. Weinzierl et al., 2011; Lieke et al., 2011) in lofted layers.

The organization of the paper is as follows. In Section 2, the measurement situation and the instrumentation are briefly described, in Section 3 we outline our methodology to derive optical properties and the volume fraction of dust. The results are discussed in detail in Section 4. A short summary concludes the paper.

*Table 1.* System parameters of the depolarization channels of the lidar systems.

| Laser | MULIS Continuum, Surelite II | POLIS Big Sky, Brillant Ultra |
|---|---|---|
| Wavelengths (nm) | 1064, 532, 355 | 355 |
| Puls energy (mJ) | 175 + 50 + 175 | 7 |
| Repetition rate (Hz) | 10 | 20 |
| Laser divergence (mrad) | 0.6 | 0.69 |
| Telescope | Cassegrain | Dall-Kirkham |
| Telescope diameter (m) | 0.3 | 175 |
| Focal length (m) | 1.2 | 0.96 |
| Field of view (mrad) | 1 to 3.5 | 2.5 |
| Detected wavelengths (nm) | 1064, $532_{par}$, 355, 607, 387, $532_{perp}$ | 355, 387 or $355_{par}$, $355_{perp}$ |
| Range resolution (m) | 7.5 | 7.5 |

## 2. Measurements and Instrumentation

To improve our knowledge about the optical, microphysical and chemical properties of Saharan dust, two field campaigns were conducted in the framework of SAMUM. The first one (SAMUM-1 – Tellus Special Issue, Volume 61, 2009) in May and June 2006 was carried out in Ouarzazate and Tinfou, Morocco, to characterize Saharan dust close to its source region. Measurements of the second campaign (SAMUM-2) were performed in 2008 at Cape Verde Islands for two reasons: first, to determine possible changes of Saharan dust within the first few days of its transport towards the Atlantic Ocean, and second to analyse Saharan dust mixed with other types of aerosols, e.g. sea salt and biomass burning aerosol. An overview of the activities during SAMUM-2 is given by Ansmann et al. (2011). The general weather conditions are described by Knippertz et al. (2011).

The Meteorological Institute MIM participated in SAMUM-2 with its two Raman- and depolarization lidar systems POLIS (Groß et al., 2008) and MULIS (Freudenthaler et al., 2009), and additionally with the sun- and sky-photometer SSARA (Toledano et al., 2009). POLIS (portable lidar system) is a small, modular, two channel lidar system. It is operating either in the Raman-mode, taking measurements of the elastic lidar return at 355 nm and of the inelastic N2-Raman shifted return at 387 nm or in the linear depolarization mode, measuring the co- and cross-polarized signals (with respect to the laser polarization plane) at 355 nm. The full overlap is at about 100 m. MULIS (multiwavelength lidar system) is a Raman- and linear depolarization lidar with elastic backscatter channels at 355, 532 and 1064 nm, and inelastic $N_2$-Raman channels at 387 and 607 nm. The linear depolarization ratio at 532 nm is derived from the co- and cross-polarized signals. MULIS' ability to scan allowed us to better observe the lowermost parts of the atmosphere. Together with the inherent low overlap of POLIS, measurements from about 100 m above ground level (note that henceforward all altitudes are given above ground level) up to the free troposphere are possible and make the combination of MULIS and POLIS an outstanding tool for observations of the PBL. The range-resolution of the raw data of both lidars is 7.5 m, and the temporal average of the raw data is 10 s. Technical details of the lidar systems are listed in Table 1.

The sun- and sky-photometer SSARA provides measurements of direct spectral radiances at twelve wavelengths between 340 and 1550 nm, and scattered radiances from the almucantar geometry. Measurements are available for the whole SAMUM-2 campaign. However, high cloudiness often prevents the evaluation of the data. Radiosondes launched twice a day by the Leibniz Institute of Tropospheric Research (IfT) provided temperature- and pressure-profiles, which are required for the calibration of the lidar signals.

Measurements of both lidar systems were performed from 14 January to 9 February 2008, whenever possible simultaneously to allow the determination of the linear depolarization ratio at two wavelengths. The typical measurement times for the lidar systems were three hours before noon (morning session) and three hours after sunset (night session). During the morning sessions POLIS operated in the depolarization mode, whereas the night sessions were performed in the Raman-mode. Furthermore, additional depolarization measurements were often performed two hours before the night sessions. We would like to point out, that the lidar ratios $S_p$ measured during the night sessions were used as input parameter for the retrieval of extinction coefficient profiles during daytime if we had sufficient

information on the temporal stability of the atmosphere. For this purpose, POLIS occasionally was operated continuously for a whole day documenting the temporal development of the aerosol distribution.

## 3. Methodology

Independent profiles of the particle extinction coefficient $\alpha_p$ and particle backscatter coefficient $\beta_p$ are retrieved from lidar signal analysis according to the Raman-method (e.g. Ansmann et al., 1992). Consequently, the extinction-to-backscatter ratio (lidar ratio) $S_p$ can be derived. As the signal-to-noise ratio of the Raman measurements is quite low due to high solar background during day, measurements of the Raman signals at 387 and 607 nm are reasonable at nighttime only. Another consequence of the low backscatter intensities is that the signals must be averaged over typically one to two hours. Note that averaging must take care of the atmosphere's temporal stability within this time slot. The resulting lidar ratios $S_p$ are used as input for the well-established analytical algorithm (Fernald, 1984) to retrieve $\alpha_p$ from the elastic signals of day time measurements. As these signals have a much better signal-to-noise ratio, a better vertical resolution of the $\alpha_p$- and $\beta_p$-profiles is provided. To investigate the temporal stability of the atmosphere between the day- and nighttime measurements (a prerequisite for the $S_p$ extrapolation) we compared profiles of the retrieved extinction coefficient (Groß et al., 2011b), of the depolarization ratio, and the lidar ratio. The AOD of the PBL is derived from the integration of $\alpha_p$-profiles assuming constant extinction below the height of full overlap.

Depolarization is described either as the volume linear depolarization ratio $\delta_v$ or the particle linear depolarization ratio $\delta_p$. The former is achieved from the co-($P_p$) and cross-polarized ($P_s$) returns according to $\delta_v = C \times P_p/P_s$ with $C$ as the calibration factor that describes the different sensitivities of the involved lidar channels. The high co-polarized signal is detected in the reflected branch of the polarizing beam-splitter cube to reduce cross-talk. Polarizing filters behind the polarizing beam-splitter additionally suppress cross-talk. The calibration factor $C$ is determined with the highly accurate $\pm 45^\circ$-calibration method described by Freudenthaler et al. (2009), either with a half-wave-plate (MULIS) or by manually rotating the channels with respect to the laser polarization (POLIS). A mechanical limit stop assures the high accuracy of the last method. The particle linear depolarization ratio $\delta_p$ is derived according to Biele et al. (2000), it depends mainly on $\delta_v$ and $\beta_p$, i.e. an inversion of the lidar signals is required before $\delta_p$ can be assessed.

The values discussed in this paper are layer integrated mean values. Although $\delta_p$ and $S_p$ are intensive parameters of the aerosols, low signal intensities lead to large uncertainties. To reduce these statistical uncertainties the layer mean values are weighted with the backscatter coefficient $\beta_p$ (see eqs 1 and 2). The error bars show the mean systematic error calculated according to Freudenthaler et al. (2009) for $\delta_p$ and Groß et al. (2011a) for $S_p$.

$$\overline{S_p} = \int_{r_1}^{r_2} \frac{\beta_p(r) \cdot S_p(r)}{\int_{r_1}^{r_2} \beta_p(r)\mathrm{d}r} \mathrm{d}r = \frac{\int_{r_1}^{r_2} \alpha_p(r)\mathrm{d}r}{\int_{r_1}^{r_2} \beta_p(r)\mathrm{d}r}. \quad (1)$$

$$\overline{\delta_p} = \int_{r_1}^{r_2} \frac{\beta_p(r) \cdot \delta_p(r)}{\int_{r_1}^{r_2} \beta_p(r)dr} \mathrm{d}r. \quad (2)$$

We also determine the volume fraction $\upsilon_d$ of dust in the PBL. For this purpose we use the ratio of the volume concentration of dust $v_d$ and all particles $v_p$ with volume concentration $v_i$ defined as volume of the particles of type "i" per volume of air, and assume only two aerosol components: dust (subscript d) and marine aerosols (subscript m).

$$\upsilon_d = \frac{v_d}{v_d + v_m}. \quad (3)$$

The volume concentration $v_i$ can be derived according to

$$\upsilon_i = \eta_i \cdot \alpha_i = \eta_i \cdot S_{p,i} \cdot \beta_i. \quad (4)$$

with $\eta_i$ being the conversion factor from extinction to volume concentration. This factor can be determined if the microphysics of the aerosols are known, in particular the size distribution, the refractive index and the particle shape. We use conversion factors published by Hess et al. (1998) in the OPAC-database. Their conversion factor for dust of $c_d = 0.905 \times 10^{-6}$ m is based on the assumption of spherical particles. Gasteiger et al. (2011) have shown that in case of non-spherical dust particles this overestimates the true value, consequently we estimate $c_d = 0.7 \times 10^{-6}$ m for our evaluations. For the marine component, we use $c_m = 0.615 \times 10^{-6}$ m according to OPAC (maritime aerosols, 70% relative humidity). The lidar ratios of dust ($S_p = 58$ sr $\pm$ 7 sr at 355 nm and $S_p = 62$ sr $\pm$ 5 sr at 532 nm) and marine aerosols ($S_p = 18$ sr $\pm$ 4 sr at 355 nm and $S_p = 18$ sr $\pm$ 2 sr at 532 nm) are taken from Groß et al. (2011b). The backscatter coefficient profiles $\beta_i$ of the two components are derived following the procedure described by Tesche et al. (2009). They found that if an aerosol ensemble consists of two components, their backscatter coefficients can be separated, provided that the linear depolarization ratios of the components are known. Adapted for our purposes, we can write for the backscatter coefficient of the dust $\beta_d$

$$\beta_d = \beta_p \frac{(\delta_p - \delta_m)(1 + \delta_d)}{(\delta_d - \delta_m)(1 + \delta_p)}. \quad (5)$$

The backscatter coefficient of the marine aerosols can easily be calculated from $\beta_m = \beta_p - \beta_d$.

The linear depolarization ratios are set to $\delta_d = 0.25$ at 355 nm and $\delta_d = 0.30$ at 532 nm for dust and $\delta_m = 0.02$ for marine aerosols at both wavelengths according to our findings from SAMUM-2 (Groß et al., 2011). With $\beta_p$ and $\delta_p$ known from our lidar measurements, we can determine $\beta_d$ according to eq.

(5). Inserting this into eq. (4) we finally derive the volume fraction of dust $\upsilon_d$ according to eq. (3). The relative uncertainties of the volume fractions are estimated to be 20–30%. They mainly result from uncertainties of the lidar measurements and retrieval, and from uncertainties of the size distribution of the particles.

For comparison we also discuss volume fractions of mineral dust and marine aerosols as derived from ground-based in situ measurements performed during SAMUM-2. In Schladitz (2011a, b) the derivation of a 'dry' dust volume fraction $\upsilon_d^{dry}$ is described. Based on this parameter, an 'ambient' volume fraction $\upsilon_d^{amb}$ is derived from numerical models using measured particle number size distribution, hygroscopic mixing state information, and hygroscopic growth factors. In Schladitz (2011a) the particle number size distribution is described by two fine modes, representing the fine portion of the marine aerosol, and two coarse modes including an external mixture of sea salt and Saharan mineral dust. Using the method described in Schladitz (2011b), the hygroscopic growth factors and hence the ambient particle number size distribution at the actual relative humidity is determined. The size resolved hygroscopic mixing state information shown in fig. 11 in Schladitz (2011a) is used to separate the hydrophobic mineral dust fraction from the ambient particle number size distribution. Subsequently, from the respective volume concentrations of the marine and the dust aerosols, ambient volume fractions of dust and marine aerosol are calculated. The temporal resolution of the retrieved data is three hours, thus somewhat lower than the remote sensing data; on the other hand they are continuously available. The relative uncertainty of the volume fractions is roughly estimated from the calculated volume concentrations to be 20%. As a conclusion, $\upsilon_d^{amb}$ is representative for the mixing state under the actual atmospheric conditions and thus, directly comparable to the volume fractions retrieved from remote sensing techniques. The dry volume fraction $\upsilon_d^{dry}$ might differ from $\upsilon_d^{amb}$ in case of hygroscopic particles and high relative humidity.

## 4. Properties of the Boundary Layer

Profiles of the relative humidity derived from the radiosonde data sets (not shown) and profiles of the optical properties from lidar measurements (Groß et al., 2011b; Tesche et al., 2011) were used to determine the height $z_{PBL}$ of the upper boundary of the PBL. It is identified by a sharp decrease of the relative humidity and a change of the extensive and intensive optical properties. As a result, we found that $z_{PBL}$ ranges between 0.3 and 0.8 km during SAMUM-2 (Fig. 1). The relative humidity within the PBL is higher than 60%, except for 6 February with a relative humidity of about 50%. Thus in all cases, sea-salt particles advected to Cape Verde from the Atlantic Ocean would still remain liquid at this relative humidity range. So we do not assume crystalline sea-salt particles in our characterization.

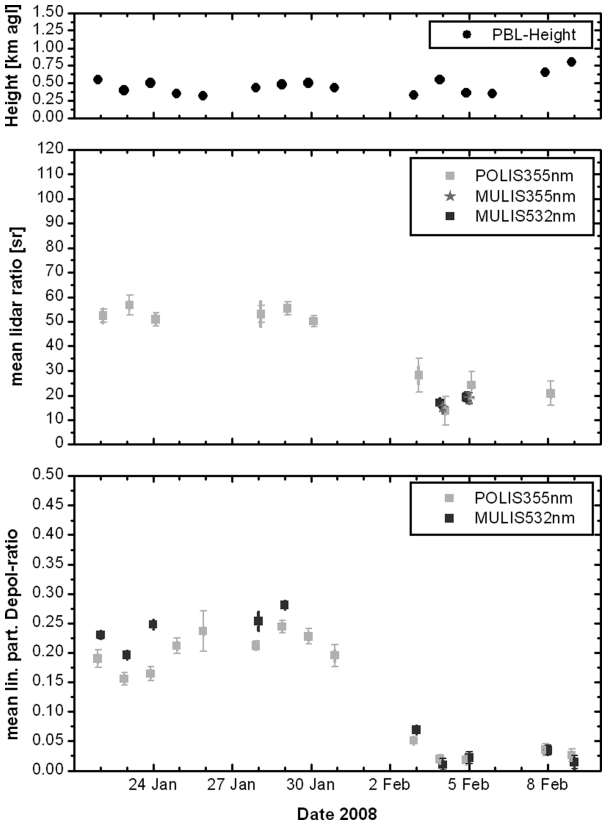


*Fig. 1.* PBL height (upper panel), and backscatter-weighted mean values of lidar ratio (middle panel) and of particle linear depolarization ratio (lower panel) in the PBL, measured with the lidar systems MULIS and POLIS. The thick lines show the standard deviation of the mean, the error bars indicate the mean systematic uncertainties.

### 4.1. Overview

As already briefly mentioned, the campaign can be divided into two phases if the characteristics of the PBL are considered. The best criterion to identify differences is the consideration of the intensive aerosol properties $S_p$ and $\delta_p$ as shown in Fig. 1. Here, we can clearly distinguish two periods: from 22 to 31 January 2008 the lidar ratio (only available at 355 nm) ranges between $50 < S_p < 55$ sr, and the $\delta_p$ values are wavelength dependent with $0.16 < \delta_p < 0.24$ at 355 nm and $0.19 < \delta_p < 0.28$ at 532 nm. The lidar ratios $S_p$ are almost as high as found for pure Saharan dust, i.e. 58 sr at 355 nm, during SAMUM-2 (Groß et al., 2011). In addition, $\delta_p$ shows high, wavelength dependent mean values similar to those of pure dust (Freudenthaler et al., 2009, Groß et al., 2011) of $\delta_p = 0.25$ at 355 nm and $\delta_p = 0.30$ at 532 nm. This is a clear indication of Saharan dust as dominating type in the PBL. In the second phase, from 3 to 9 February, $S_p$ in the PBL is significantly lower than during the first period, with wavelength independent values of $14 < S_p < 27$ sr only, indicating a dominance of spherical particles, probably wet sea-salt particles. This assumption is confirmed by the analyses of

*Table 2.* Summary of the mean lidar ratios $S_p$, particle linear particle depolarization ratios $\delta_p$, and dominant aerosol type of the two identified time periods at 355 nm from POLIS measurements and at 532 nm from MULIS measurements.

| Date | $S_p$ mean (sr) | | $S_p$ range (sr) | | $\delta_p$ mean | | $\delta_p$ range | | Dominant type |
|---|---|---|---|---|---|---|---|---|---|
| | 355 nm | 532 nm | 355 nm | 532 nm | 355 nm | 532 nm | 355 nm | 532 nm | |
| 22.01.–31.01. | 54 | – | 50 – 59 | – | 0.20 | 0.24 | 0.16–0.24 | 0.19–0.28 | Saharan dust |
| 3.01.–9.01. | 21 | 18 | 14 – 27 | 17 – 19 | 0.03 | 0.03 | 0.02–0.05 | 0.01–0.07 | Sea-salt |

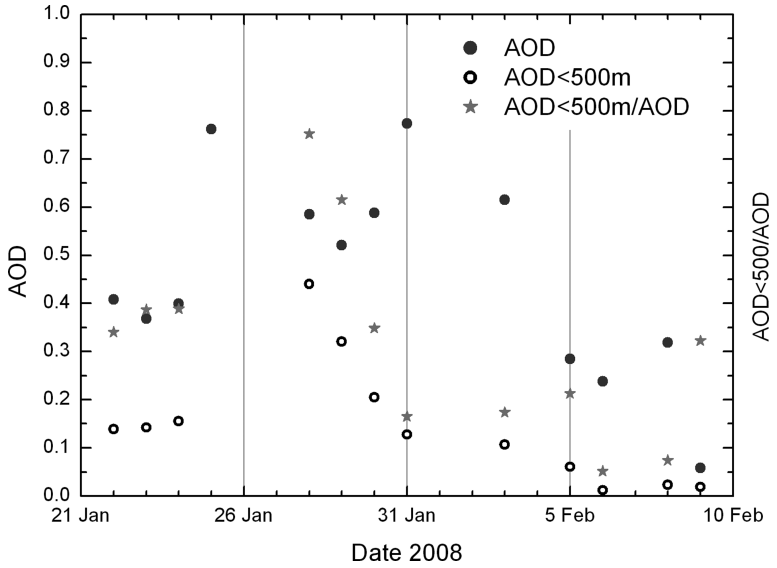


*Fig. 2.* Daytime mean aerosol optical depth at 340 nm (AOD – dark grey dots) derived from SSARA sun-photometer measurements, AOD at 355 nm below 0.5 km height (AOD < 500 m – dark grey circles) calculated from POLIS lidar measurements, and relative contribution of the AOD below 0.5 km height to the total AOD (light grey stars).

$\delta_p$, where we find low values of $0.02 < \delta_p < 0.05$ at 355 nm and $0.01 < \delta_p < 0.07$ at 532 nm. An overview of the most relevant intensive aerosol properties of the PBL for the two time periods is given in Table 2. It includes the mean values of $S_p$ and $\delta_p$, as well as their maximum and minimum values.

The discrimination of the two episodes is not so clear considering only the total optical depth. Figure 2 shows daily averages of the AOD ($\tau$) derived from the SSARA sun-photometer measurements at 340 nm, and the AOD in the lowermost 500 m ($\tau_{500}$) calculated from POLIS lidar measurements at 355 nm. The latter quantity is a simplification as it applies a constant height range, but it was chosen to have the same representative and comparable parameter of the PBL for the whole campaign. Furthermore, the ratio of both quantities $\varepsilon = \tau_{500}/\tau$ is given to describe the relative contribution of the PBL to the total AOD at 355 nm. For this purpose, we calculated the total AOD at 355 nm from SSARA measurements at 340 nm using the Angström exponent between 340/500 nm. Missing values are either due to high cloudiness or the absence of daytime lidar measurements. Figure 1 shows a large variability of the vertical integrated properties—of the absolute as well as of the relative quantities. During the first phase of the measurements the AOD of the PBL varies between $\tau_{500} = 0.13$ on 31 January and $\tau_{500} = 0.44$ on 28 January, and the relative contribution $\varepsilon$ ranges between 17% and 76%. During the second phase of the SAMUM-2 campaign (3–9 February) the relative contribution of the lowermost 500 m ranges between 5% and 32%. The values of $\tau_{500}$ between 0.02 on 9 February and 0.1 on 3 February are considerably lower than during the first period.

Note that the time periods identified on the basis of the lidar measurements conform with the general weather situation as described in Knippertz et al. (2011) where they found higher wind velocities during the second phase, and therefore good conditions for sea-salt aerosol production

### *4.2. Case studies*

In this section, we want to focus not only on the optical properties of the aerosols in the PBL but also on the quantitative assessment of the volume fraction of dust in the PBL. For this purpose we discuss in depth representative time slices from three days, two of them from the first phase.

#### *22 January 2008*

The first period we selected for a detailed analysis is 22 January 2008, 16–17 UTC. Analyses of POLIS measurements show an AOD in the lowermost 500 m of $\tau_{500} = 0.14$. This is about 34% of the total AOD at 355 nm. The PBL height determined from profiles of the relative humidity and lidar derived optical

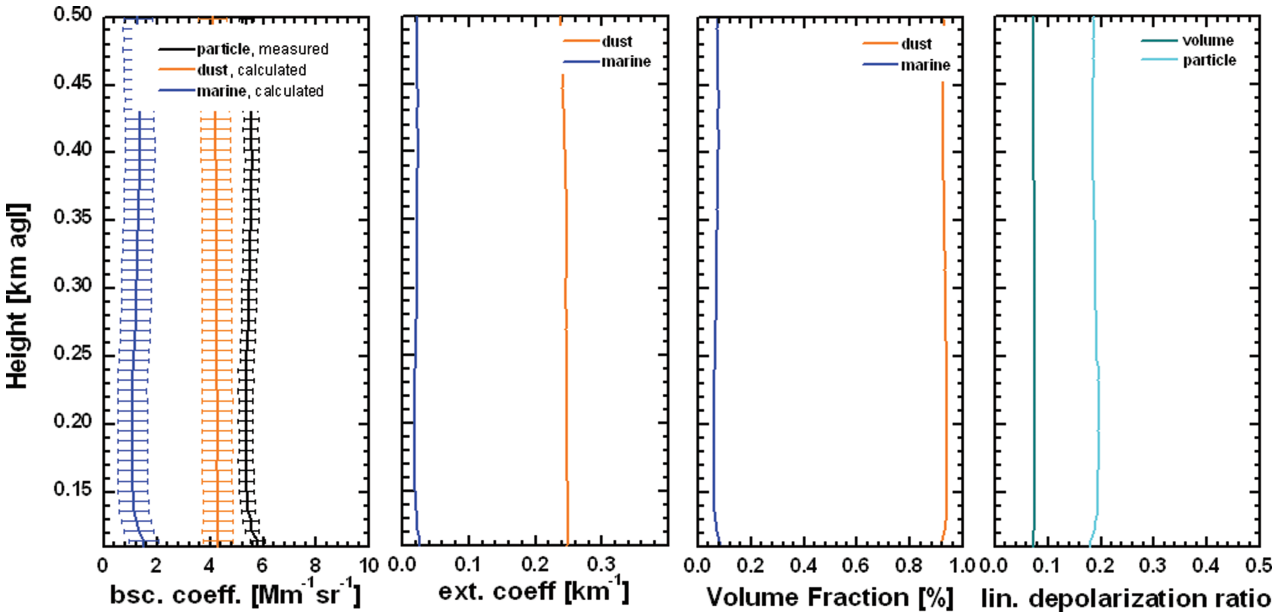


*Fig. 3.* Dust (orange line), marine (blue line) and total backscatter coefficient, dust and marine extinction coefficient, both at 355 nm, volume fraction of dust and marine aerosols, and measured volume and particle linear depolarization ratio (from left to right) on 22 January 2008 between 16:00 and 17:00 UTC.

properties is $z_{PBL} = 550$ m. The relative humidity in the PBL is about 60%. The mean lidar ratio of this layer is $S_p = 52$ sr $\pm$ 3 sr (note that the $\pm$ range denotes the mean systematic uncertainty) at 355 nm and thus similar to lidar ratios of dust.

An overview of the height dependent (measured) parameters that are relevant for the assessment of the volume fraction of dust $\upsilon_d$ as well as the retrieved profiles of $\upsilon_d$ and $\upsilon_m$ are shown in Fig. 3. The rightmost panel shows the profile of $\delta_p$ (355 nm), the parameter that is essential according to eq. (5) to derive the backscatter coefficient profiles $\beta_d$ of dust and $\beta_m$ of marine aerosols (first panel). With respect to the backscatter coefficient, dust is contributing with roughly 80% to the total. The volume linear polarization ratio $\delta_v$ is included as it is required for the calculation of $\delta_p$ (rightmost panel). The PBL during the considered time period is well mixed, consequently the polarization ratios are almost height independent throughout the PBL with a mean linear particle depolarization ratio $\delta_p$ of $0.19 \pm 0.02$ at 355 nm and $0.23 \pm 0.01$ at 532 nm. This points to a high amount of non-spherical dust particles. As described in the previous section the extinction coefficients $\alpha_d$ and $\alpha_m$ (second panel) are calculated applying adequate lidar ratios. The extinction due to dust was $\alpha_d = 0.25$ km$^{-1}$, compared to only 0.02 km$^{-1}$ of marine aerosols. Finally, the volume fractions of dust and marine aerosols are derived (see third panel). They exhibit a very high dominance of dust in the PBL with $\upsilon_d = 93\%$.

These results were compared to the volume fractions derived from the ground-based in situ measurements of a 3-h sample between 12 UTC and 15 UTC, and from the single particle analysis (Kandler et al., 2011a). Under dry conditions the in situ measurements give volume fractions of dust of $\upsilon_d^{dry} = 92\%$ and consequently $\upsilon_m^{dry} = 8\%$ for the marine component. Calculation of the ambient volume fraction results in $\upsilon_d^{\text{amb}} = 83\%$. The difference can be attributed to hygroscopic growth of the marine particles. The single particle analysis results in a volume fraction of Saharan dust of $\upsilon_d = 89\%$ (dry conditions). As a conclusion, the findings from the in situ analyses and from the remote sensing approach are in good agreement.

### *30 January 2008*

On 30 January 2008 the AOD of the PBL is $\tau_{500} = 0.2$, corresponding to about 35% of the total AOD. The PBL layer height is $z_{PBL} = 500$ m and the relative humidity in the PBL ranges between 60% and 70%. The mean $S_p$ and $\delta_p$ values at 355 nm are 50 sr $\pm$ 2 sr and $0.22 \pm 0.01$, respectively, again indicating a high amount of non-spherical dust particles. Analogue to Fig. 3, POLIS measurements of the particle backscatter coefficient, and of the volume and particle depolarization ratios, that are required for the retrieval of the volume fractions, are shown in Fig. 4. They are based on two-hour averages from 18 to 20 UTC. The retrieved profiles of the dust and marine aerosols ($\beta_d$ and $\beta_m$, $\alpha_d$ and $\alpha_m$) as well as the calculated volume fractions $\upsilon_d$ and $\upsilon_m$ are also plotted in Fig. 4. It can be seen that the dominance of dust was even higher than on 22 January: the dust contributes more than 90% to the particle backscatter coefficient (leftmost panel). The dust related extinction coefficient is $\alpha_d \sim 0.40$ km$^{-1}$, whereas the marine aerosol related extinction coefficient is virtually negligible with $0.01 < \alpha_m < 0.02$ km$^{-1}$. Accordingly, the

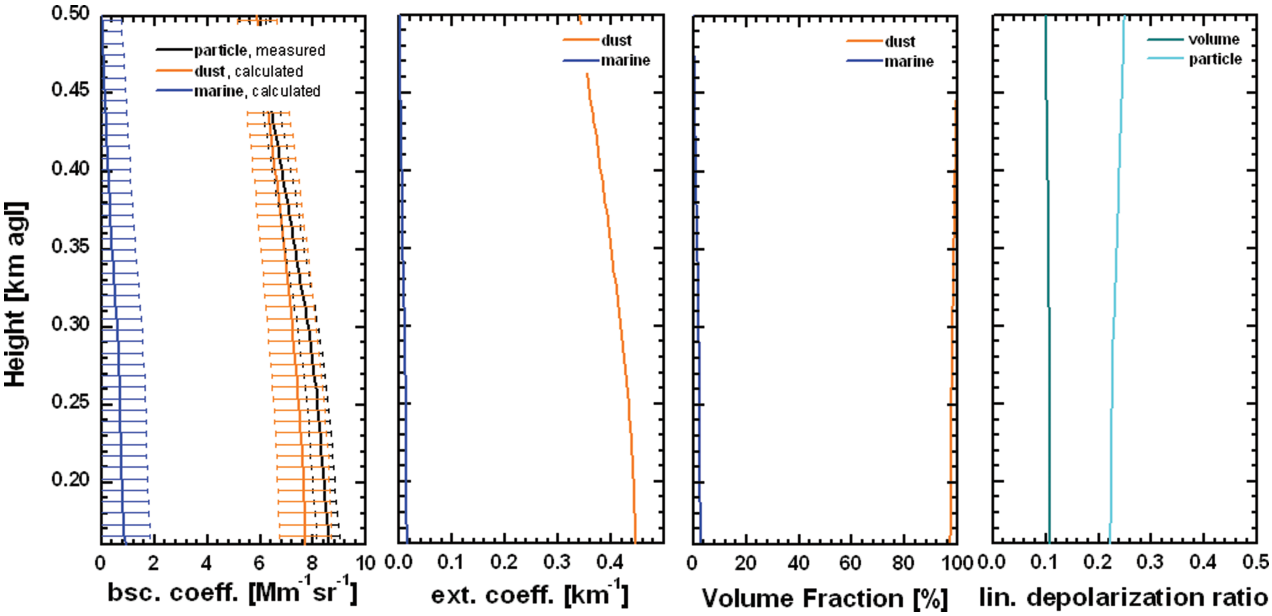


*Fig. 4.* Same as Fig. 3 but for 30 January 2008, 18:00–20:00 UTC.

dust contribution to the total volume of the PBL $\upsilon_d$ is 98%, the marine aerosols' contribution is only 2%.

This result is in perfect agreement with the outcome of the single particle analysis, that results in $\upsilon_d = 98\%$ for the volume fraction of dust. Comparison with the in situ measurements, sampled between 18 UTC and 21 UTC, reveals $\upsilon_d^{dry}$ and $\upsilon_d^{amb}$ to be 99% for the Saharan dust contribution.

### *3 February 2008*

From the second phase, we selected 3 February for a detailed analysis and considered the two-hour interval from 17:30 to 19:30 UTC. The PBL height is $z_{PBL} = 300$ m. The AOD of the PBL, $\tau_{500}$, with $\tau_{500} = 0.10$ is considerably lower than on the days discussed before. The contribution to the total AOD is about 20%. As already briefly mentioned the intensive values of the aerosols in the PBL show differences to the days discussed above. The mean values of $S_p$ are wavelength independent with $S_p = 28$ sr $\pm$ 7 sr. Mean $\delta_p$-values are $\delta_p = 0.05 \pm 0.01$ at 355 nm and $\delta_p = 0.07 \pm 0.01$ at 532 nm, respectively. These values indicate a high contribution of spherical particles. As before, the profiles of the measured backscatter coefficient, the volume and particle linear depolarization ratios, the calculated backscatter and extinction coefficients of dust and marine aerosols, and the resulting volume fractions are shown in the four panels of Fig. 5. As already expected from inspection of the $\delta_p$-profiles, the retrieval of the dust and marine volume fractions in the PBL reveals completely different results than the previous cases: with $\upsilon_d = 42\%$ and $\upsilon_m = 58\%$ both components are almost equally contributing.

Comparing these values to the results from the in situ sampling from 18 to 21 UTC, we see very good agreement with the ambient volume fraction of dust ($\upsilon_d^{amb} = 39\%$), but significant differences when the dry volume fraction, which is much higher with $\upsilon_d^{dry} = 66\%$, is considered. This effect may be explained with the hygroscopicity of marine aerosols (e.g. Tang et al., 1997). From Wise et al. (2005) we estimate an increase of 60% of the volume equivalent radius of marine aerosols due to hygroscopic growth for the meteorological conditions of Praia during SAMUM-2, i.e. relative humidity in the range of 60–70% and transport of marine particles from the sea, where higher humidity is likely. In contrast, the Saharan dust particles are not hygroscopic. The consequences with respect to $\upsilon_d$ are illustrated in Fig. 6, where $\upsilon_d$ under dry and ambient conditions is plotted. If the volume fraction of Saharan dust $\upsilon_d$ in the PBL is large, the difference between $\upsilon_d^{amb}$ and $\upsilon_d^{dry}$ is small, because virtually all particles are hydrophobic. With decreasing $\upsilon_d^{dry}$, which is equivalent to an increasing amount of hygroscopic (marine) particles, the ambient volume fraction of dust $\upsilon_d^{amb}$ decreases even stronger.

To elaborate the implications of hygroscopic growth on aerosol mixtures consisting of hydrophobic and hygroscopic components – in our case dust and marine aerosols – and to compare the available methodologies, we show the different time series of our analyses over the whole measurement period in Fig. 7. Shown are the dry and ambient volume fractions of dust derived from the ground based in situ measurements – data that are available almost continuously, the retrievals from the single particle analysis, and the volume fractions calculated from our lidar measurements. Note that the lidar retrievals include 12

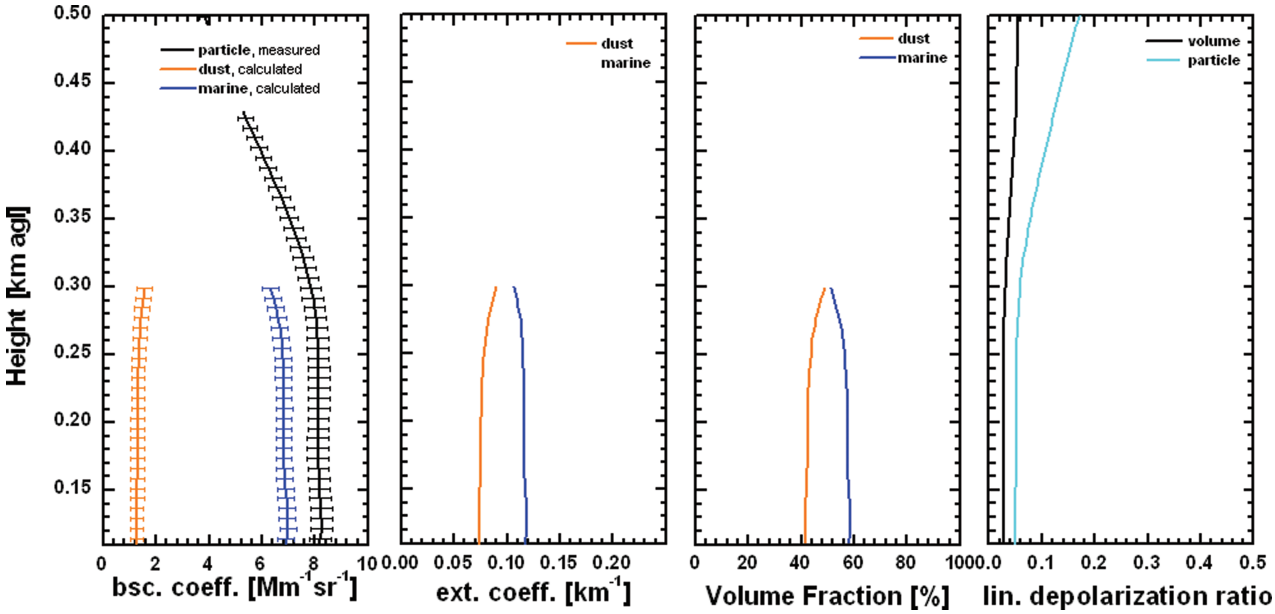


*Fig. 5.* Same as Fig. 3 but for 3 February 2008, 17:30–19:30 UTC.

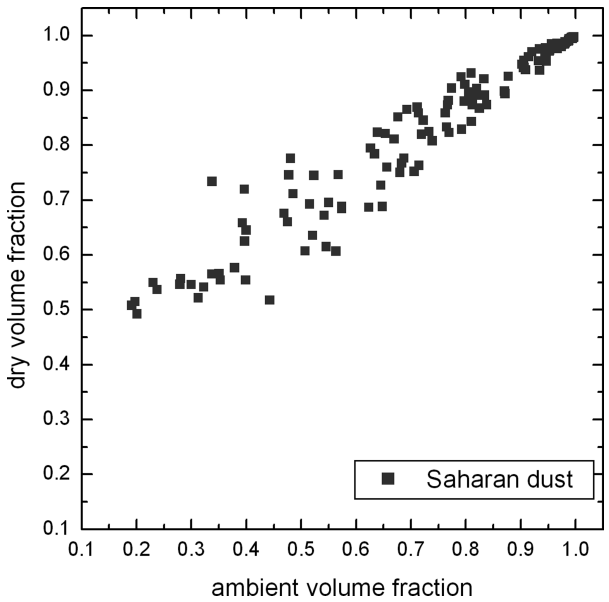


*Fig. 6.* Dry volume fraction of Saharan dust versus ambient volume fraction derived from in situ measurements at Praia, Cape Verde from 20 January to 9 February 2008. Each point describes a three hour sample.

cases at 355 nm and 6 cases at 532 nm in total, thus more than the 3 case studies discussed earlier.

Three features are of special relevance. First, it is clearly visible, that at the beginning of February the aerosol regime changed from a dust-dominated mixture to a mixture with significant contribution of marine aerosols. This change was already found from the intensive aerosol properties from the lidar measurements (Fig. 2). However, the temporal coverage of the in situ measurements is better so that the time of the change can be assessed more accurately. Second, it is obvious that the dry volume fraction is always equal or greater than the ambient volume fraction (derived from the in situ measurements). This is a consequence of the underlying physical concept that under conditions of high relative humidity a certain number of the non-dust aerosols grow. The reduction of the volume fraction of dust during the second part of the experiment is much more pronounced than during the first part. This fact is consistent with the higher amount of marine aerosols. The third feature is the very good general agreement of the different retrievals. In this context it is noteworthy that the agreement of the retrieval based on the lidar measurements with the ambient volume fraction is much better than with the dry volume fraction, as expected from the physical processes. For the same reason $\upsilon_d$ from the single particle analysis agrees better with the dry volume fraction from the in situ data.

Slight differences between $\upsilon_d$ from the lidar retrieval and the ambient volume fraction (in situ) are only observed when the contribution of dust was low, i.e. $\upsilon_d^{amb} < 30\%$ (5, 6 and 9 February). On these days in situ measurements reveal a larger dust volume fraction than the lidar measurements. A possible reason for this discrepancy is the relative large error of the retrievals when $\upsilon_d$ is low. Another reason is that the lowermost hundred meters cannot be observed by the lidars in spite of the low overlap of POLIS and the fact that MULIS measurements under low elevation angles were considered in the evaluation. Under conditions with a high marine component in the PBL this very shallow height range might become relevant: as the wind speed is high (Knippertz et al., 2011), the production of

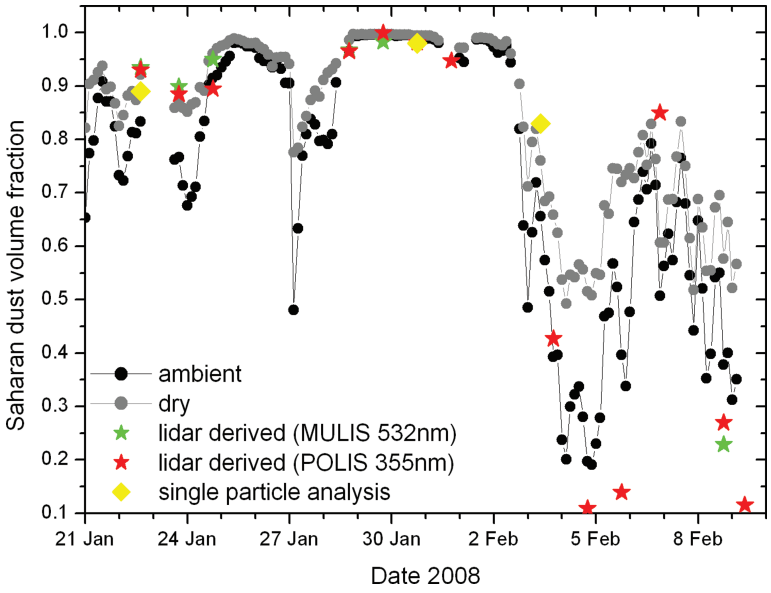


*Fig. 7.* Volume fraction of Saharan dust in the PBL over Praia, Cape Verde, from 21 January–9 February 2008. The black dots show the in situ measurements under ambient relative humidity, the grey dots in situ measurements of the dry volume fraction. The single particle analysis, as well as the lidar derived volume fractions are indicated by yellow rectangles, and green and red stars, respectively.

dust with large particles (radius larger than 10 $\mu$m) from local sources might be enhanced and accumulate in this layer (Kandler et al., 2011b). As a consequence, a vertical gradient of aerosol properties builds up, leading to differences between the ground based aerosol samples and the atmospheric volume that is sensed by the lidar. This effect is in particular relevant on days with a low background concentration of Saharan dust as during the last days of the campaign.

## 5. Summary and conclusion

This paper focuses on the investigation of aerosols in the PBL over Cape Verde conducted in the framework of SAMUM-2 from 21 January till 9 February 2008. On the one hand we determined intensive optical properties from lidar measurements that are known to be suited to characterize aerosol particles: the lidar ratio $S_p$ and the linear depolarization ratio $\delta_p$. On the other hand, we present a novel approach to derive the volume fractions of dust $\upsilon_d$ and marine aerosols $\upsilon_m$ based on lidar measurements. This approach is based on high quality measurements of $\delta_p$. The results were compared to independent in situ measurements.

On the basis of the lidar derived optical characterization the field campaign could be divided into two phases with respect to the presence of dust in the PBL. Colocated sun-photometer data support this classification, though it was partly masked by the inherent vertical integration. During the first phase, the PBL was dominated by hydrophobic Saharan dust particles. Calculations of the volume fraction of dust agree very well with in situ measurements of the volume fraction at ambient relative humidity. The agreement with the dry volume fraction was also good as the majority of the particles are hydrophobic. During the second phase, the dry and ambient volume fraction of the in situ measurements differ, as during this episode the abundance of hygroscopic marine aerosols was significant. We found (not unexpectedly) that this effect gets larger with an increasing fraction of marine aerosols. So the assessment of $\upsilon_d$, its interpretation, and the comparison between different measurement techniques (in situ versus remote sensing) must take into account the ambient relative humidity and the hygroscopicity of the particles.

It should be mentioned that the assessment of $\upsilon_d^{amb}$ involves several evaluation steps and assumptions, thus we estimate the relative errors to be in the range of 20–30%, both for the lidar retrieval as well as for the in situ measurements. The methodology in general is based on the assumption of an aerosol mixture of two components, one of which being hydrophobic and one hygroscopic. The lidar retrieval relies on the prescribed linear depolarization ratios of the two pure components, which is not a critical issue in our case, as these numbers are known with high accuracy from our previous measurements. Furthermore, the methodology requires lidar systems that are capable to measure as close to the ground as possible – an overlap of 500 m or even more is certainly not acceptable for the characterization of the PBL. Our lidar systems fulfil this requirement, as the overlap is not more than 100 m. The assessment of $\upsilon_d^{amb}$ by means of in situ measurements is among others influenced by the accuracy of the assumed hygroscopic growth factors and information on the hygroscopic mixing state.

In this paper we have demonstrated, that from lidar measurements the volume fraction of dust in the PBL can be derived. As the lidar systems of the Meteorological Institute of the LMU provide lidar depolarization ratios at two wavelengths, $\lambda = 355$ and 532 nm, the investigation of the potential of an extension of the methodology is envisaged in a next step. This extension might either increase the accuracy of the derived volume fractions in case of a two-component aerosol mixture (e.g. dust and

marine aerosols), or makes it possible to adapt the approach for more component mixtures. The extension of our retrieval of volume fractions to a retrieval of mass fractions is expected to be easily feasible, as only the mass density of the aerosols has to be known. The knowledge of mass fractions can be quite important with respect to air quality and flight safety.

## 6. Acknowledgments

The SAMUM research group is funded by the Deutsche Forschungsgemeinschaft (DFG) under grant 539.

## References

Ansmann, A., Wandinger, U., Riebesell, M., Weitkamp, C. and Michaelis, W. 1992. Independent measurement of extinction and backscatter profiles in cirrus clouds by using a combined raman elastic-backscatter lidar. *Appl. Opt.* **31**, 7113.

Ansmann, A., Petzold, A., Kandler, K., Tegen, I., Wendisch, M. and co-authors. 2011. Saharan Mineral Dust Experiments SAMUM-1 and SAMUM-2: what have we learn? *Tellus* **63B**, this issue.

Biele, J., Beyerle, G. and Baumgarten, G. 2000. Polarization lidar: corrections of instrumental effects. *Opt. Express* **7**, 427–435.

Fernald, F. G. 1984. Analysis of atmospheric lidar observations: some comments. *Appl. Opt.* **23**, 652–653.

Freudenthaler, V., Esselborn, M., Wiegner, M., Heese, B., Tesche, M. and co-authors. 2009. Depolarization ratio profiling at several wavelengths in pure saharan dust during samum 2006. *Tellus* **61B**, 165–179.

Gasteiger, J., Groß, S., Freudenthaler, V. and Wiegner, M. 2011. Volcanic ash from Iceland over Munich: massconcentration retrieved from ground-based remote sensing measurements. *Atmos. Chem. Phys.* **11**, 2209–2223, doi:10.5194/acp-11-2209-2011.

Groß, S., Freudenthaler, V., Toledano, C., Seefeldner, M. and Wiegner, M. 2008. Mini-lidar measurements of particle depolarization and Raman scattering of Saharan-dust and biomass burning at 355 nm during SAMUM 2, *Proc. Of 24th International Laser Radar Conference*, Boulder, USA, 23–27 June 2008, S04P-10.

Groß, S., Wiegner, M., Freudenthaler, V. and Toledano, C. 2011a. Lidar ratio of Saharan dust over Cape Verde Islands: assessment and error calculation. *J. Geophys. Res.*, doi:10.1029/2010JD015435, in press.

Groß, S., Tesche, M., Freudenthaler, V., Toledano, C., Wiegner, M. and co-authors. 2011b. Characterization of Saharan dust, marine aerosols and a mixture of biomass burning aerosols and dust by means of multi-wavelength depolarization- and Raman-measurements during SAMUM 2. *Tellus* **63B**, this issue.

Hess, M., Köpke, P. and Schult, I. 1998. Optical properties of aerosols and clouds: the software package OPAC. *Bull. Am. Meteorol. Soc.* **79**, 831–844.

Hooper, W. P. and Eloranta, E. W. 1986. Lidar measurements of wind in the planetary boundary layer: The method, accuracy and results from joint measurements with radiosonde and kytoon. *J. Clim. Appl. Meteorol.* **25**, 990–1001.

Kandler, K., Lieke, K., Benker, N., Küpper, M., Emmel, C. and co-authors. 2011a. Electron microscopy of particles collected at Praia, Cape Verde, during the Saharan Mineral dust experiment: particle chemistry, shape, mixing state and complex refractive index. *Tellus* **63B**, this issue.

Kandler, K., Schütz, L., Jäckel, S., Lieke, K., Emmel, C. and co-authors. 2011b. Ground-based off-line aerosol measurements at Praia, Cape Verde, during the Saharan Mineral Dust Experiment: Microphysical properties and mineralogy. *Tellus* **63B**, this issue.

Kiemle, C., Ehret, G., Giez, A., Davis, K.J., Lenschow, D. H. and co-authors. 1997. Estimation of boundary layer humidity fluxes and statistics from airborne differential absorption lidar (dial). *J. Geophys. Res.* **102**, D24, 29189–29203

Knippertz, P., Tesche, M., Heinold, B., Kandler, K., Toledano, C. and co-authors. 2011. Dust Mobilization and Aerosol Transport from West Africa to Cape Verde-A Meteorological Overview of SAMUM-2. *Tellus* **63B**, this issue.

Kunkel, K.E., Eloranta, E.W. and Shipley, S.T. 1977. Lidar observations of the convective boundary layer. *J. Appl. Meteorol.* **16**, 1306–1311.

Lieke, K., Kandler, K, Emmel, C., Petzold, A., Weinzierl, B. and co-authors. 2011. Particle chemical properties in the vertical column based on aircraft observations 1 in the vicinity of Cape Verde, *Tellus* **63B**, this issue.

Matthias, V. and Bösenberg, J. 2002. Aerosol climatology for the planetary boundary layer derived from regular lidar measurements, *Atmos. Res.* **63**, 221–245.

Melfi, S. H., Spinhirne, J. D., Chou, S.-H. and Palm, S. P. 1985. Lidar observations of vertically organized convection in the planetary boundary layer over the ocean. *Am. Meteorol. Soc.* **24**, 806–821.

Murayama, T., Okamoto, H., Kaneyasu, N., Kamataki, H. and Miura, K. 1999. Application of lidar depolarization measurement in the atmospheric boundary layer: effects of dust and sea-salt particles. *J. Geophys. Res.* **104**, D24, 31,781–31,792.

Schladitz, A., Müller, T., Nowak, A., Kandler, K., Lieke, K. and co-authors. 2011a. In situ aerosol characterization at Cape Verde, Part 1: particle number size distributions, hygroscopic growth and state of mixing of marine and Saharan dust aerosol. *Tellus* **63B**, this issue.

Schladitz, A., Müller, T., Nordmann, S., Tesche, M., Groß, S. and co-authors. 2011b. In situ aerosol characterization at Cape Verde, Part 2: parametrization of relative humidity- and wavelength-dependent aerosol optical properties. *Tellus* **63B**, this issue.

Schwiesow, R. L. 1984. A comparative overview of active remote-sensing techniques. In *Probing the Atmospheric Boundary Layer* (ed. Lenshow, D. H.). American Meteorological Society.

Strawbridge, K. and Snyder, B. 2004. Planetary boundary layer height determination during pacific 2001 using the advantage of a scanning lidar instrument. *Atmos. Environ.* **38** (34), 5861–5871. Available at: http://dx.doi.org/10.1016/j.atmosenv. Accessed 2003.10.065.

Stull, R. B. 1988. *An Introduction to Boundary Layer Meteorology*. Kluwer Academic, Dordrecht.

Tang, I. N., Tridico, A. C. and Fung, K. H. 1997. Thermodynamic and optical properties of sea salt aerosols. *J. Geophys. Res.* **102**, D19, 23, 269–23,275.

Tesche. M., Ansmann, A., Müller, D., Althausen, D., Engelmann, R. and co-authors. 2009. Vertically resolved separation of dust and smoke over Cape Verde by using mulitwavelength Raman and polarization lidars during Saharan Mineral Dust Experiment 2008. *J. Geophys. Res.* **114**, doi:10.1029/2009JD011862.

Tesche, M., Groß, S., Ansmann, A., Müller, D., Althausen, D. and co-authors. 2011. Profiling of Saharan dust and biomass burning smoke with multiwavelength polarization Raman lidar at Cape Verde. *Tellus* **63B**, this issue.

Toledano, C., Wiegner, M., Garhammer, M., Seefeldner, M., Gasteiger, J. and co-authors. 2009. Spectral aerosol optical depth characterization of desert dust during samum 2006. *Tellus* **61B**, 216–228.

Toledano, C., Wiegner, M., Groß, S., Freudenthaler, V., Gasteiger, J. and co-authors. 2011, Optical properties of aerosol mixtures derived from sun-sky radiometer during SAMUM-2. *Tellus* **63B**, this issue.

Weinzierl, B., Sauer D., Esselborn M., Petzold A., Veira A. and co-authors. 2011. Microphysical and optical properties of dust and tropical biomass burning aerosol layers in the Cape Verde region—an overview of the airborne in situ and lidar measurements during SAMUM-2. *Tellus* **63B**, this issue.

Wiegner, M., Emeis, S., Freudenthaler, V., Heese, B., Junkermann, W. and co-authors. 2006. Mixing layer height over Munich, Germany: variability and comparisons of different methodologies, *J. Geophys. Res.* **111**, D13201, 17, doi:10.1029/2005JD006593.

Wise, M.E., Biskos, G., Martin, S.T., Russell, L.M. and Buseck, P.R. 2005. Phase transitions of single salt particles studied using a transmission electron microscope with an environmental cell. *Aero. Sci. Technol.* **39**, 849–856.